sustainability

MDPI

Article

Pyrolytic Conversion of Vomitoxin-Contaminated Corn into Value-Added Products

Shokooh Karami, Sadegh Papari, Naomi B. Klinghoffer * and Franco Berruti

Institute for Chemicals and Fuels from Alternative Resources (ICFAR), Department of Chemical and Biochemical Engineering, Faculty of Engineering, Western University, London, ON N6A 5B9, Canada
* Correspondence: nklingh@uwo.ca; Tel.: +1-519-661-2111 (ext. 86981)

Abstract: Deoxynivalenol (DON) (also called vomitoxin) is a mycotoxin caused by pathogens that periodically contaminate crops such as maize, wheat, barley, oats, and rye, making them unusable. We explored pyrolysis as a process for the decontamination of vomitoxin-corn grains and their transformation into value-added products. Pyrolysis was carried out in a bench-scale batch reactor at maximum temperatures between 450 and 650 °C. This resulted in the total destruction of DON, from 5–7 ppm in raw corn grains to non-detectable levels in the treated bio-char. The effect of pyrolysis conditions, including temperature and heating rate, on the conversion of toxic corn grains was investigated. The maximum bio-oil yield was achieved at 650 °C (47 wt.%). The co-products were bio-char (29 wt.%) and non-condensable gases (24 wt.%). Acetic acid and levoglucosan were the two major valuable components in the bio-oil, corresponding to 26 g/kg and 13 g/kg of bio-oil, respectively. The bio-chars were analyzed and upgraded by physical activation using CO_2 at 900 °C. Activation increased the bio-char surface area to 419 m^2g^{-1} and promoted pore development, which was verified by SEM. Proximate analysis illustrated that stable carbon increased to 88.8% after activation compared to 10.9% in the raw corn. FT-IR results showed that the thermally unstable functional groups had been completely eliminated after activation. All characterization results confirmed that the activated corn bio-char has excellent potential for adsorption processes. The HHV of the non-condensable gas stream was 16.46 MJ/Nm^3, showing the potential application of this product as an energy source.

Keywords: deoxynivalenol (DON); corn grain; pyrolysis; activated bio-char; adsorption

Citation: Karami, S.; Papari, S.; Klinghoffer, N.B.; Berruti, F. Pyrolytic Conversion of Vomitoxin-Contaminated Corn into Value-Added Products. *Sustainability* **2022**, *14*, 12842. https://doi.org/10.3390/su141912842

Academic Editor: Maurizio Volpe

Received: 10 August 2022
Accepted: 29 September 2022
Published: 8 October 2022

1. Introduction

Maize is one of the most important agricultural products in terms of production, consumption, and economic importance. In addition to being a source for human food, it is used for animal feed, and as feedstock for biofuel production [1,2]. Its production keeps increasing, for example, according to the Food and Agriculture Organization (FAO), maize production increased significantly in the United States from 250 million tonnes in 2000 to about 350 million tonnes in 2018. Its contamination with deoxynivalenol (DON) generally occurs in countries with humid climates, such as the United States, Europe, and Canada [3,4]. Deoxynivalenol (DON) (also called vomitoxin due to the strong vomiting effect after consumption [5]) is a mycotoxin substance produced by pathogens such as *Fusarium graminearum* (*Gibberella zeae*), and *Fusarium culmorum*, contaminating crops such as maize, wheat, barley, oats, and rye [5,6]. DON affects human and animal health, causing food refusal, vomiting, suppression of the immune system, abdominal pain, and diarrhea [2].

Table 1 shows DON concentrations in maize from 2011 to 2020 in Ontario, Canada. In 2018, more than half of Ontario's corn was infected with DON due to high humidity that summer, and only 33% of corn produced that year contained less than 0.5 ppm of

DON. Furthermore, 25% of corn contained vomitoxin levels above 5 ppm, which is the maximum allowable limit for pig feed [7].

Table 1. Fluctuations of DON concentrations in maize occurred in Ontario over a period of ten years (produced using data from [8]).

DON Concentration (ppm)	Percentage (%)									
	2011	**2012**	**2013**	**2014**	**2015**	**2016**	**2017**	**2018**	**2019**	**2020**
<0.5	47	84	83	66	75	48	69	33	84	58
0.5 to <2	28	12	15	26	20	26	17	27	12	31
2 to <5	17	4	1	6	5	18	8	15	4	10
5 and greater	7	0	0	2	0	8	6	25	0	0

Many studies discussed different solutions for decontamination of the toxic maize and possible outcomes (Table 2). Figure 1 schematically illustrates the possible remediation or detoxification methods for corn grains, which can be categorized as physical, chemical, and biological treatments. In some instances, combinations of these processes can be used. Washing or steeping can be effective for water-soluble toxins such as DON.

Trenholm et al. [9] and Sinha [10] studied the effect of washing on the DON-concentration changes in contaminated corn, and the results show up to 67% reduction. Another study by Bullerman and Bianchini showed a 19% DON reduction in corn using sorting, trimming, and cleaning [11]. Chemical treatments for mycotoxin corn have also been widely studied. but there are only a few implementations of this due to the complications of treated products for human consumption. Cazzaniga et al., [12] showed that sodium bisulfite is effective at reducing DON concentrations. However, alteration of the corn's structure makes this product suitable only for animal feed. A recent study performed in 2021 discussed the effect of ozone as a chemical treatment for removing DON. The results showed a 41% reduction after 180 min, indicative of achieving the difficult degradation of DON only after long contact times [13]. No chemical or enzymatic treatments have been approved by the European Union for mycotoxin treatments due to the extensive need for safety testing after treatments and possible structural and chemical changes in the products [2].

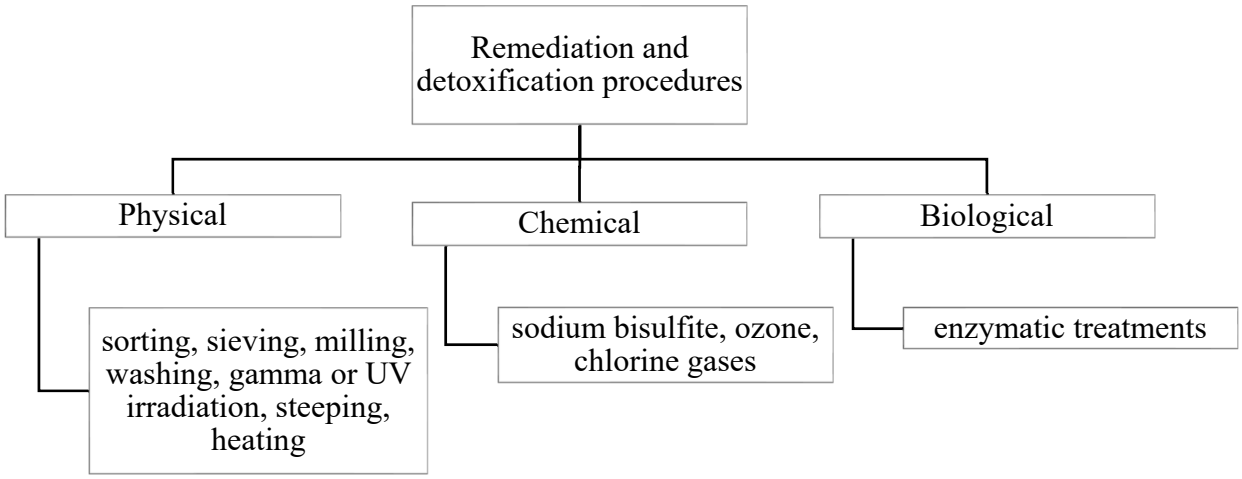

Figure 1. Remediation and detoxification methods for DON-contaminated corn (produced with information from reference [2]).

Table 2. Summary of various techniques used for the decontamination of DON from maize.

Process	Year	Condition	Results	Drawbacks
Chemical and physical treatment [14]	1986	(1) Moist ozone (1.1 mol %) in air (2) 30% chlorine	(1) 90% of DON reduction after an hour (2) Total destruction of DON after 0.5 h	-
Washing [9]	1992	Washing three times with DI water, using sodium carbonate solution (1 M)	73% of DON reduction	Expensive post-treatments such as drying after decontamination
Cooking [12]	2001	Extrusion process at 180 °C, adding sodium metabisulfite (1%)	95% of DON reduction	-
Bt corn [4]	2004	Using Bt corn as a genetically modified crop	Annual loss reduced from $52 to $8 million	The majority of Bt corn is used for animal feed
Food processing [11]	2007	Sorting, trimming, and cleaning	DON concentration reduction from 5.5% to 19%	These processes do not fully destroy DON structure
Ozone [13]	2021	In contact with Ozone for 180 min	42% of DON reduction	DON appeared to be quite difficult to degrade even at elevated contact times

Biomass is currently drawing considerable attention as a renewable resource for the production of materials and energy [15]. The environmental advantages (e.g., low carbon footprint), abundance, and continuous renewal, as well as the waste-reduction potential make it a sustainable alternative to fossil resources [16]. Although the total replacement of fossil fuels with biomass is impossible in the near future, multiple approaches are being pursued for the production of value-added products from residual biomass and waste. Many studies are at the research and development level, but several have already achieved commercial implementation [17]. There are several pathways for biomass conversion from various feedstocks (i.e., woody products, such as forestry wastes and bark; agricultural products, such as purpose grown crops, residues, and manure; and organic wastes, such as industrial and municipal organic fractions) to chemicals and fuels. These include biological, thermal, and mechanical (physical) processes. The most common thermochemical conversion processes are pyrolysis, combustion, gasification, and liquefaction. Pyrolysis has the advantage of being a relatively fast process, not requiring intensive feedstock pre-treatments [18], and generating valuable products that have applications in the agricultural, pharmaceutical, and chemical industries [19,20]. Therefore, non-edible DON-contaminated corn was targeted as a potential biomass feedstock for the pyrolysis process.

This study represents an original contribution towards investigating the feasibility of using pyrolysis for the destruction of DON in corn grains as a potential solution for managing this seasonal waste. Through this process, waste is converted into value-added products such as bio-char, bio-oil, and non-condensable gases, which have various industrial applications. This pathway for converting this non-edible feedstock has not been explored previously.

2. Materials and Methods

2.1. Feedstock

Field-contaminated corn grain samples were obtained from the Grain Farmers of Ontario in Guelph, Ontario, Canada and used as the feedstock for this work. The concentra-

tion of deoxynivalenol (DON) in the feedstock was measured by SGS Canada Inc., Hensall, Ontario, using an Enzyme-Linked Immunoassay (ELISA), Diagnostix, EZ-TOX DON (with a detection limit of 0.5 ppm) and was found to be between 5 and 7 ppm. The proximate analysis of the raw corn (Table 3), providing the amounts of volatile matter (VM), fixed carbon (FC), and ash), based on ASTM D1762, showed a high percentage of volatile content. The ultimate analysis, on an ash-free basis, (Table 3) indicated a nitrogen percentage (1.34%) higher than typical lignocellulosic wastes (0.5–1.0%) [21], offering promising opportunities for the production of bio-char with fertilizer properties. The higher heating value was measured using a bomb calorimeter. According to the US Food and Drug Administration (FDA), the maximum acceptable DON levels for human and animals consumption are shown in Table 4 [7].

Table 3. Proximate and ultimate analysis of raw corn.

	Raw Corn
Proximate analysis (wt.%)	
Moisture	8.2
Volatiles	79.9
Fixed Carbon (By difference)	10.9
Ash	0.97
Ultimate analysis (wt.%)	
C	41.1
H	6.22
N	1.34
S	0
O (By difference)	51.3
High heating value (MJ kg^{-1})	16.0

Table 4. Maximum allowable DON levels in human and animal food according to FDA (ppm).

Human	**Ruminating Beef, Feedlot Cattle, and Chickens**	**Swine**	**All Other Animals**
1	10	5, not to exceed 50% of the diet	5, not to exceed 40% of the diet

2.2. Experimental Setup

Slow pyrolysis experiments were performed in a batch pyrolysis reactor with mechanical mixing, as illustrated in Figure 2. Whole corn grains were put directly into the reactor without any pre-processing. The reactor consisted of a 316 stainless steel horizontal cylinder 33 cm long and 20 cm in internal diameter, with a capacity of 8.5 L. The reactor used an internal rotating paddle mixer to achieve good mixing of the reacting feedstock and, consequently, good heat transfer and effective conversion [22]. The reactor was heated using an induction furnace (5–100 KW, Superior Induction Company, Pasadena, CA, USA) with an on–off controller connected to a thermocouple inside the reactor. The pressure inside the reactor was measured using a pressure gauge (max 15 psi) connected to a pressure-release valve (McMaster-Carr, Cleveland, OH, USA). There was no sweep gas present, and the product flow was driven by the pressure differential produced by the products. A stainless-steel shell and tube condenser kept in a water bath (filled by tap water) was used to collect the condensable vapors (bio-oil). Non-condensable gases exiting the condenser would then pass through a cotton filter (replaced regularly as needed), after which samples were collected in a gas bag or directed to the exhaust line. A summary of the operating conditions is shown in Table 5. Once the system reache the maximum temperature, it was held at that temperature for 30 min, and then the heating was turned

off. To investigate the adsorption potential of bio-char as a substitute for commercial activated carbons derived from fossil fuels, samples of bio-char produced at different temperatures were subsequently physically activated using a SS316 tubular reactor with 5 cm O.D and 100 cm length. A 240-volt electric tube furnace (Lindberg/Blue M, Ashville, NC, USA) was used to heat the reactor. The activation was performed under CO_2 at 900 °C for 3 h.

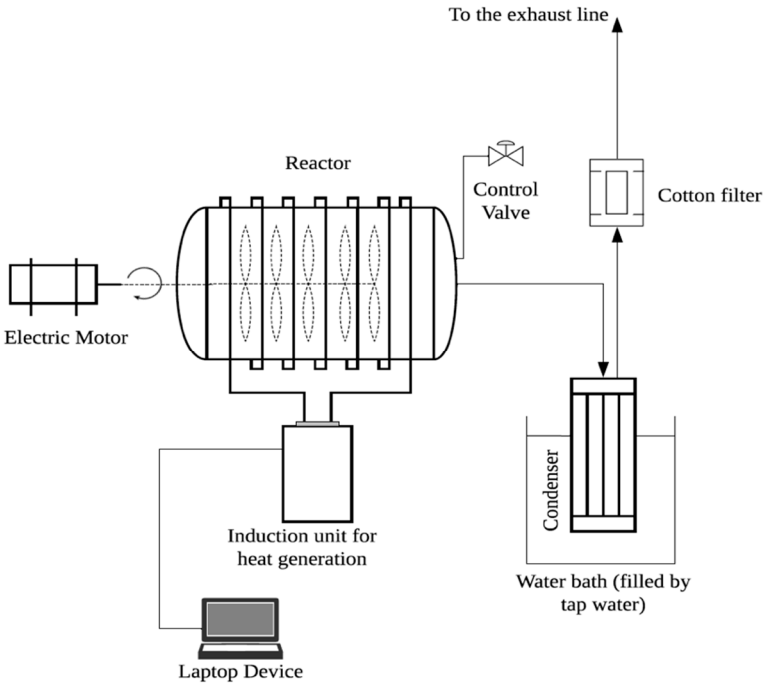

Figure 2. Process Flow Diagram (PFD) of the horizontal mechanically mixed pyrolysis reactor.

Table 5. Pyrolysis operating conditions during parametric testing of temperature in batch system.

Pyrolysis Operating Conditions	
Temperature	450 to 650 °C in 50 °C increments
Pressure	1 atm
Feedstock	500 g
Mixer speed	30 to 40 rpm
Heating rate	20 °C/min
Condenser	Room temperature (20 °C)

2.3. Feedstock and Products Characterization Methods

2.3.1. Gas Chromatography–Mass Spectrometry (GC-MS)

The GC-MS system comprises a gas chromatograph coupled to a quadrupole mass spectrometer (GC-MS QP 2010, Shimadzu) using a capillary column (DB-5MS, 30 m × 0.25 mm i.d.; film thickness, 0.25 μm). The ion source temperature and interface temperature of the Electron ionization (EI) was maintained at 200 °C and 250 °C, respectively. While using EI, the instrument was initially used in SCAN mode to acquire the identity of the compounds. The GC system was equipped with a split/spitless inlet. An AOC-20S autosampler with a 10 μL syringe was employed to inject 1 μL of sample at a rate of 10 μL s^{-1}. Helium (UHP) was the carrier gas entering the system at a constant flow of 1.5 mL min^{-1}. The oven temperature program had an initial temperature of 40 °C, which was held for 10 min and then increased by 10 °C/min to 200 °C. This was held for 10 min and increased with the same heating rate of 10 °C/min to reach 300 °C. The sample was held for

another 30 min, with a total run time of 75 min. This temperature was selected to provide an effective separation of the compounds of interest.

2.3.2. High Performance Liquid Chromatography (HPLC)

The concentration of the main components, i.e., sugars, organic acids, furfural, 5-HMF, alcohols, and acetol, were determined using a Shimadzu high performance liquid chromatography (HPLC), using external standards for identification and quantification of peak areas. These components were quantified using an Agilent Hi-plex H (7.7 × 300 mm) column (Agilent USA, Santa Clara, CA, USA) and RID-10A detector.

2.3.3. Thermogravimetric Analysis (TGA)

TGA tests were performed using the Pyris 1 TGA Thermogravimetric Analyzer (PerkinElmer, Waltham, MA, USA) available at Surface Science Western (Western University). In each experiment, 5 mg of the sample was heated from 30 °C to 300 °C with a heating rate of 10 °C min^{-1} and nitrogen flow rate of 50 mL min^{-1}. The sample was held at 300 °C for 30 min, and the temperature was then raised to 700 °C with 15 °C min^{-1} ramp rate and held for 5 min.

2.3.4. Infrared Spectroscopy (FTIR)

Small portions of the samples were analyzed using Fourier Transform Infrared (FTIR) spectroscopy using the Platinum® attenuated total reflectance (Pt-ATR) attachment equipped with a diamond crystal in the main box of a Bruker Tensor II spectrometer, Coventry, England. This experimental setup allowed us to analyze an area of approximately 2 mm × 2 mm to a depth of 0.6–5 microns. The spectra were collected from 4000–400 cm^{-1} with a resolution of 4 cm^{-1} and 32 scans.

2.3.5. Surface-Area (BET) Measurements

Surface-area measurements for bio-char and activated bio-char samples were obtained using the Brunauer-Emmett-Teller (BET) method. This was carried out using a Nova 1200e Surface Area & Pore Size Analyzer (Quantachrome Instrument, Boynton Beach, FL, USA). A total of 0.3 g of each sample was subjected to tests by nitrogen gas sorption at 77.35 K.

2.3.6. Scanning Electron Microscopy (SEM) Analysis and Energy Dispersive X-ray Analyses

The SEM-EDX analysis of the raw biomass and bio-char samples was performed using the Hitachi SU3500 Scanning Electron Microscope (SEM) combined with an Oxford AZtec X-Max50 SDD energy dispersive X-ray (EDX) detector available at Surface Science Western (Western University). Backscatter Electron (BSE) imaging was used to provide a superior analysis of the particles, with variations in greyscale based on the average atomic number of the material. EDX is a semi-quantitative technique capable of detecting all elements with a minimum detection limit of approximately 0.5 wt.%. An accelerating voltage of 10-kV was used for these analyses. The samples' surfaces were coated with a thin layer of gold to minimize any charging effects.

2.3.7. Micro Gas Chromatography (Micro-GC)

A Varian Micro-GC (CP-4900) equipped with MS5 Å (Molecular Sieve 5 Å, 10 m), PPU (PolarPlot U, 10 m) and 5 CB (CP-Sil 5 CB, 8 m) column modules was used to analyze the concentration of H_2, CH_4, CO, CO_2, C_2H_4, C_2H_6, C_3H_6, C_3H_8, and C_4H_{10}. The gas components from each sample were detected over a period of 3.0 min and automatically integrated using Galaxie software, version 1.9.302.530.

3. Results and Discussion

3.1. DON Concentration in Products

DON concentration in the samples, including bio-oil at 450 °C, 550 °C, and 650 °C and activated bio-chars, were measured using ELISA, Diagnostix, EZ-TOX DON (detection limit 0.5 ppm). The analysis found that the DON concentration is less than 0.5 ppm in all samples, which is negligible.

3.2. Production Yields

Effect of Temperature and Heating Rate

The effect of temperature and heating rate on the product yields from the slow pyrolysis of contaminated corn are shown in Figures 3 and 4. The bio-char and bio-oil yields were measured by weight, and the gas yield was calculated by difference. The bio-oil yield increased (from 30% to 46%) as the final pyrolysis target temperature increased from 450 °C to 650 °C, while the bio-char yield decreased (from 42% to 24%). Duplicate experiments confirmed the accuracy of the results, as shown in the figures. The gas yield remained almost constant over all experiments. Higher pyrolysis temperatures typically accelerate the cracking reactions that produce bio-oil, resulting in lower char production. This trend is aligned with previous studies utilizing corn starch as feedstock [23,24]. The heating rates tested ranged from 5 °C min^{-1} to 35 °C min^{-1}. The effect of the heating rate was similar to the effect of temperature on the yield of products. Bio-oil production increased at higher heating rates, while char production decreased.

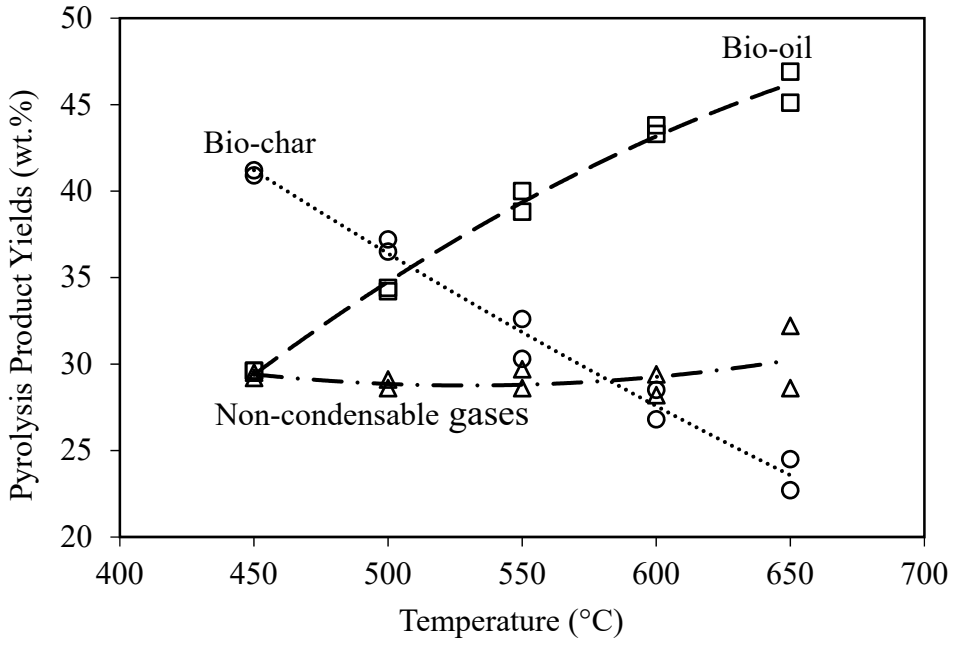

Figure 3. Effect of final target temperatures on the pyrolysis product yields (holding time at T_{max}: 30 min, heating rate: 20 °C min^{-1}).

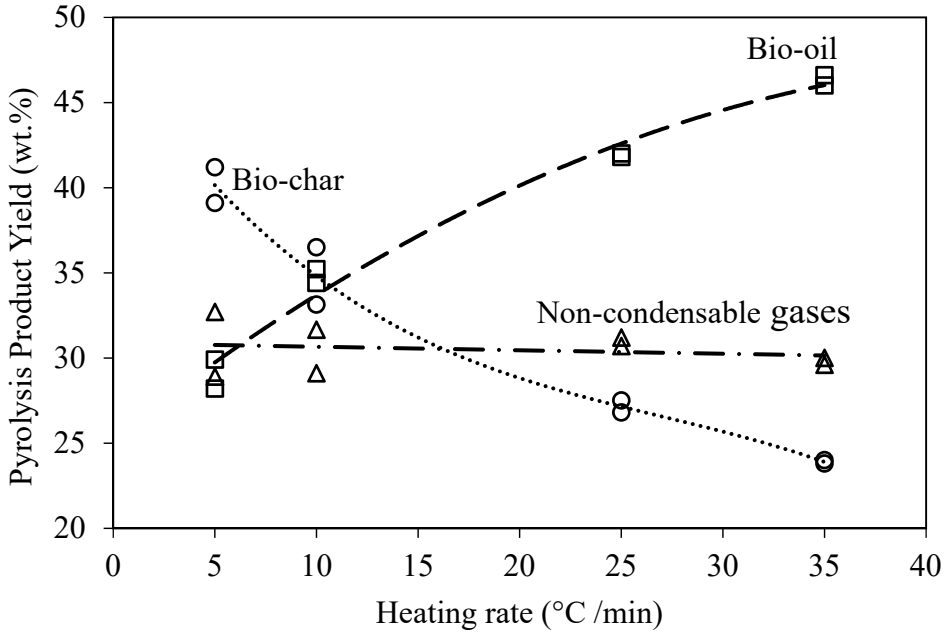

Figure 4. Effect of heating rate on the yields of products (holding time at T_{max}: 30 min, target temperature: 500 °C).

3.3. Bio-Oil Product Characterization

3.3.1. GC-MS Analysis

GC-MS analysis was performed on the bio-oils produced at final target temperatures between 450 °C and 650 °C. The bio-oil mainly consisted of an aqueous phase with only a thin organic layer on top. The sample taken for GC-MS analysis represents both phases after being mechanically mixed. Table 6 shows the primary components that were identified in the GC-MS. As is evident from Table 6, the peak areas were highest for acetic acid, followed by levoglucosan and furfural (at lower temperatures). The acetic acid peak area percentage was 51% at 450 °C and 54% at 500 °C. However, at higher temperatures, the acetic acid percentage remained constant at 47%. The highest peak area percentage of levoglucosan was 20% at 650 °C, and the highest percentage of furfural was 10% at 500 °C.

Table 6. Chemical constituents of bio-oil identified by GC-MS.

Compounds	Peak Area (%) Temperature (°C) *				
	450	**500**	**550**	**600**	**650**
Acetic acid	50.72	54.23	47.28	47.09	47.34
Propanoic acid	1.62	ND	1.27	1.45	1.63
Furfural	7.40	10.40	4.05	ND	ND
5-methyl-2-Furancarboxaldehyde	4.48	4.13	2.20	1.34	1.14
3,3-dimethyl-2-Butanone	2.21	1.85	2.20	1.15	1.09
1-(acetyloxy)-2-Butanone	1.85	1.56	1.25	0.87	0.81
2-hydroxy-3-methyl-2-cyclopenten-1-one	2.82	3.06	ND	ND	ND
Maltol	1.62	1.71	1.52	0.50	0.57
1,4:3,6-Dianhydro-.alpha.-d-glucopyranose	4.07	3.18	5.90	4.60	3.68
levoglucosan	6.69	4.32	4.87	15.94	20.16
Phenol	1.38	1.14	2.31	2.90	1.93
2-Furanmethanol	1.49	ND	1.38	1.53	1.87

ND: Not detected. * heating rate of 20 °C/min.

The peak percentages provided by the GC-MS analysis are only an approximate indication of the relative concentrations of the different main components identified, which were subsequently quantified by HPLC. Figure 5 reports the concentrations of the five main components in the bio-oil produced at different target pyrolysis temperatures. The highest yield of acetic acid, which was 26 g/kg of bio-oil, occurred at 500 °C. Levoglucosan was the second major component and showed the highest yield of around 13 g/kg of bio-oil at 650 °C.

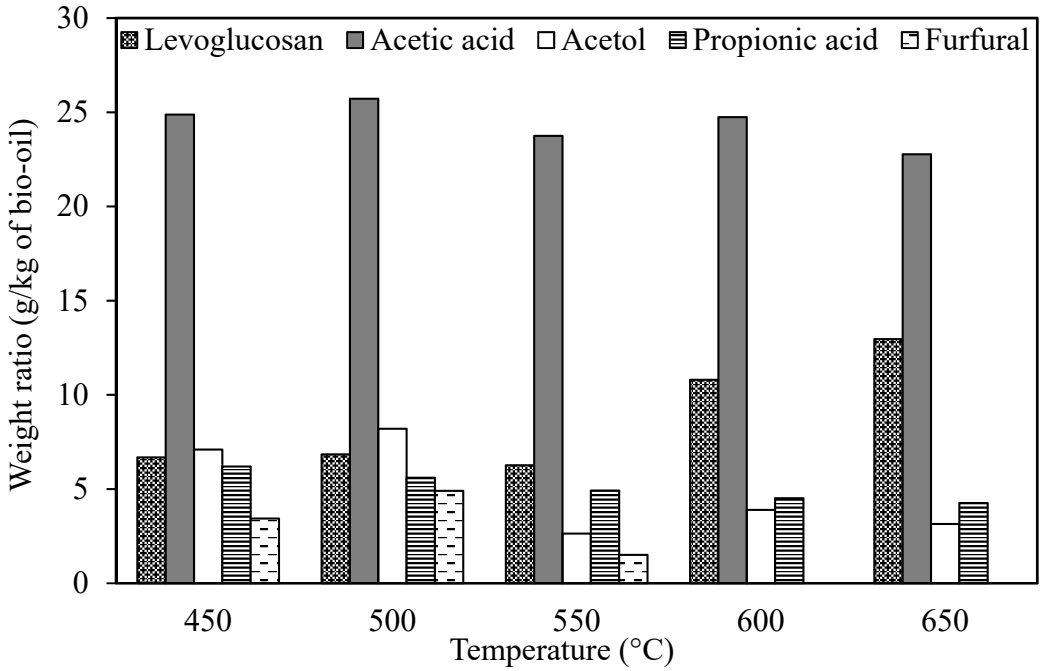

Figure 5. Weight ratio of the components (g/ kg of bio-oil) recognized in the bio-oil using HPLC.

3.3.2. Bio-Oil Evolution during Slow Pyrolysis

To better understand the production of condensable vapors during the slow batch pyrolysis, bio-oil was collected at selected intermediate temperatures (between 300 and 550 °C) as the temperature increased from ambient to 550 °C (Figure 6). The results show that the rate of bio-oil production is approximately constant during the overall batch pyrolysis process. The GC-MS results showed levoglucosan had the maximum peak at 350 °C (28%), while acetic acid's maximum peak (60%) occurred at 500 °C (Figure 7).

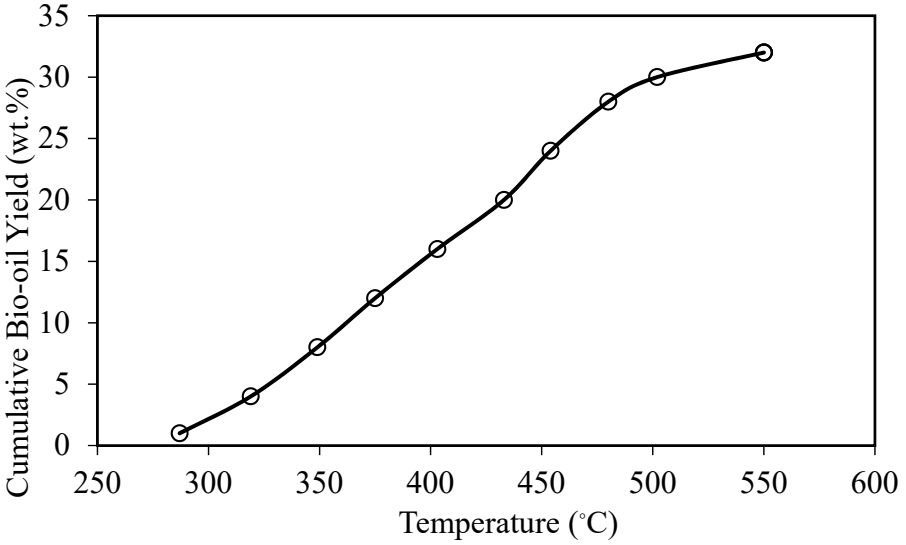

Figure 6. Bio-oil yield progression with increasing reaction temperature (from 300 to 550 °C).

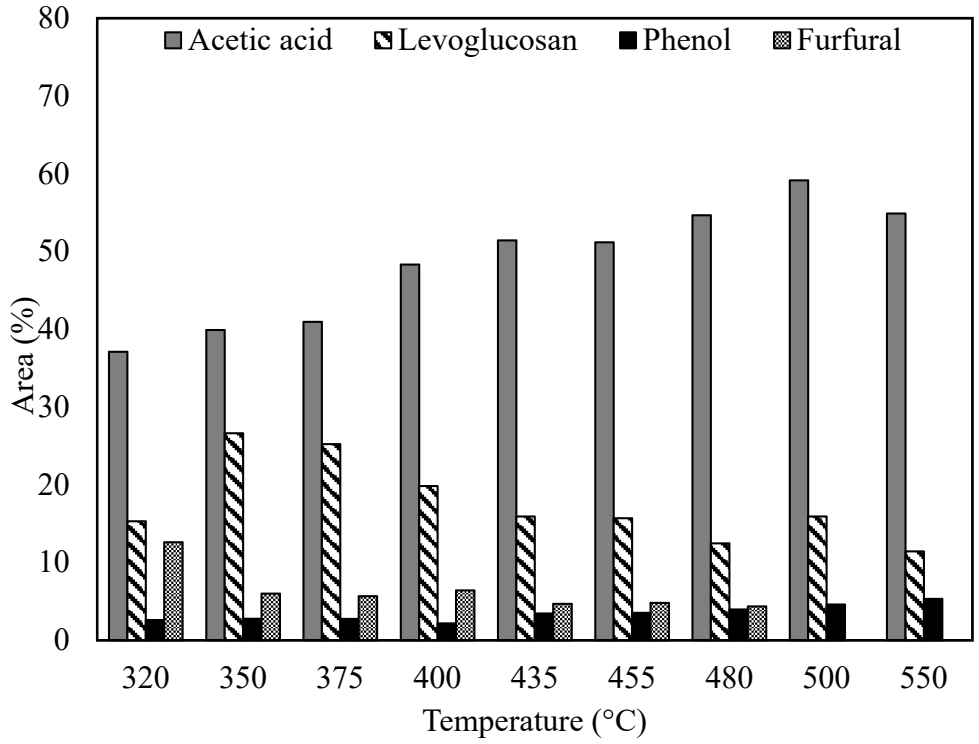

Figure 7. Bio-oil composition at nine different temperatures between 320 and 550 °C by GC-MS.

3.4. Bio-Char Characterization

The hydrogen and oxygen contents of the bio-chars decreased as the pyrolysis temperature increased, while the carbon and ash contents increased with increasing temperatures (Table 7). The highest amount of fixed carbon, which was 81.8%, was observed at 650 °C. The decrease in oxygen and hydrogen content is due to the cracking of weak bonds at higher temperatures, producing H_2O, CO, and CO_2 [25]. Compared to woody and grassy feedstocks, which contain less than 1% nitrogen [16,21], corn biomass has a higher nitrogen content of 2%, making it more attractive as a potential fertilizer for soil amendment applications.

Table 7. The effect of pyrolysis temperature on the characteristics of bio-char and activated bio-char (proximate and CHNS analysis).

	Temperature (°C)					
	450	**500**	**550**	**600**	**650**	**Activated Bio-Char at 900 °C for 3 h**
Proximate analysis (wt.%)						
Moisture	1.95	1.89	1.88	2.8	2.54	0.95
Volatiles	49.87	32.55	24.9	15.38	7.33	4.17
Fixed Carbon (By difference)	44.09	60.94	67.5	74.13	81.77	88.11
Ash	4.09	4.62	5.72	7.69	8.36	6.77
Ultimate analysis (wt.%)						
C	72.56	73.16	75.66	79.12	82.65	84.0
H	3.94	4.19	3.34	2.47	1.49	1.49
N	2.20	1.75	2.14	2.3	2.44	1.53
S	0	0	0	0	0	0
O (By difference)	21.30	21.62	18.86	16.11	13.42	12.98
H/C	0.05	0.06	0.04	0.03	0.02	0.02
O/C	0.29	0.30	0.25	0.20	0.16	0.15
pH	6.19	6.26	6.69	7.28	7.45	8.98
High heating value (MJ kg^{-1})	23.67	27.75	28.48	30.44	29.55	-

3.4.1. Thermogravimetric Analysis (TGA)

In order to understand thermal degradation behavior, thermogravimetric analysis (TGA) was performed on biomass (raw corn), on bio-char produced at 450 to 650 °C, and on activated corn bio-char (ACB-3h). The DTG curve in Figure 8 shows that moisture loss was observed around 80 °C, followed by another major weight loss at 300 °C (45% reduction) caused primarily by the starch decomposition reactions. Such weight loss occurs at temperatures lower than those typical of lignocellulosic feedstocks.

Qiao et al., 2019 [19] studied the pyrolysis of corn starch, and the results showed that major decomposition during corn starch pyrolysis takes place between 320–354 °C. This is due to its structure. Corn is mainly composed of starch (70%) and proteins (10%) [26]. The TGA results match the work conducted by Yang et al. on maize [24]. According to these studies [19,24], the main decomposition of corn starch happens between 300 °C and 400 °C, which correspond to the temperature range of the starch thermal decomposition.

Figure 8 illustrates that activated bio-char (ACB-3h) and bio-char (BC-650) experience a small weight loss between 300 to 400 °C, corresponding to a slight downward trend (~5%). During pyrolysis at temperatures above 600 °C, the majority of the volatiles and starch are removed from the bio-char structure; therefore, the biochar does not experience significant weight loss, as observed in the TGA. However, bio-chars produced at lower temperatures (BC-450 and BC-550) show significant weight loss, i.e., 35% and 15%, respectively. This is likely due to the higher content of volatiles than are present in these biochar samples.

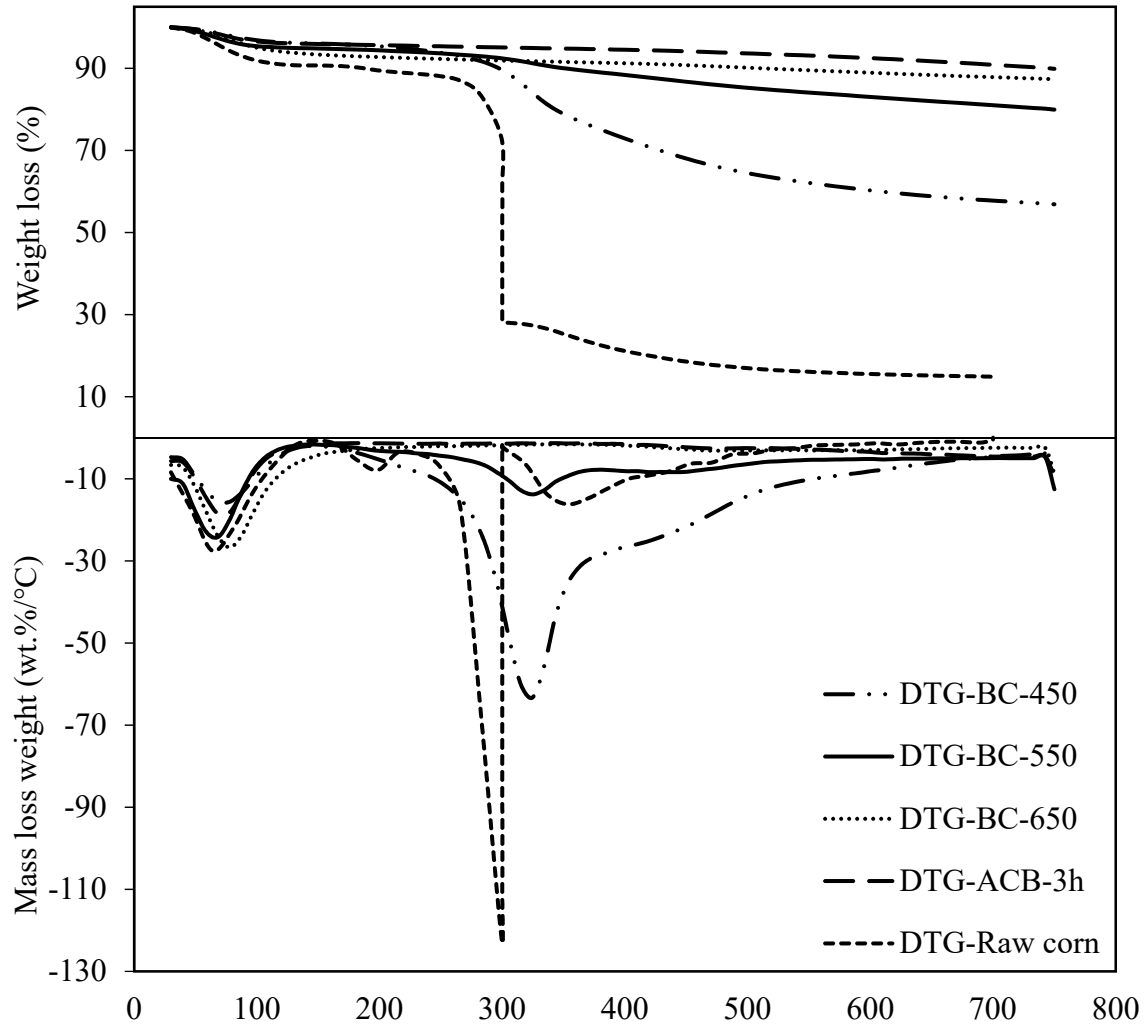

Figure 8. TGA and DTG results for raw corn, bio-char (BC) produced at 450, 550, and 650 °C (holding time: 30 min) and activated bio-char with activation holding time of 3 h (ACB-3h).

3.4.2. FTIR

FTIR is used for both the structural determination of organic compounds and for bio-char bond description [16]. Figure 8 shows the FTIR patterns for raw corn and bio-char products. Table 8 shows the wavenumbers corresponding to the main peaks and the functional groups attributed to each region. In the corn starch spectrum, O–H, CH_2, and –C–C– stretching vibrations are attributed to wavenumbers of 3200–3400, 2850–2900, and 1600–1700 (cm^{-1}), respectively. For raw corn, the peaks with 1300–1450 cm^{-1} and 850–900 cm^{-1} wavenumbers represent O–H and –C–C–bending vibration [27]. Raw corn displays the highest number of peaks at the single-bond and fingerprint regions. The changes show that, at higher temperatures, the intensity of light components (3252 cm^{-1} band) with hydroxyl (–OH) and carboxyl (–COOH) groups decreases for bio-char at 450 °C. These components disappear at higher temperatures. Raw corn has two peaks with high absorbance intensity of 3252 cm^{-1} and 1014 cm^{-1}, showing the presence of a high number of alcohols, hydroxyls, and aliphatic compounds in its structure compared to other samples. As the temperature increases, only complex compounds within the fingerprint region remain. For example, two peaks of 1581 cm^{-1} and 868 cm^{-1} show the aromatic rings, and 1155 cm^{-1} shows the amine compounds with CN stretch. This finding is aligned with the ratio of

H/C and O/C from the elemental analysis illustrated in Table 7. These two ratios decrease by increasing the temperature [28], which confirms the disappearance of light components. Figure 9 illustrates that complex compounds such as aromatics and aliphatics can be seen even at high temperatures (900 °C). The results are in accordance with studies by A. R. Oromiehie et al. [27] and Kizil et al. [29].

Table 8. FTIR peaks analysis (adapted from [30]).

Spectrum Region	Region Wavenumber Range (cm^{-1})	Wavenumber (cm^{-1})		Functional Group/Assignment
		Experiment	Literature	
Single bond (O-H, N-H, C-H)	4000–2500	3252	3400–3200	Alcohol and hydroxyl, OH stretch
			3300–3030	Ammonium ion, NH_4^+
		2919	2935–2915	Methylene, (>CH2) stretch
		2847	2865–2845	
Triple bond (C≡C, C≡N)	2500–2000	No peak was observed	-	-
Double bond (C=C, C=O, C=N)	2000–1500	1581	1615–1580	Aromatic ring stretch, C=C–C
			1630–1575	(–N=N–)
		1328	1410–1310	Phenol or tertiary alcohol, OH bend
Fingerprint	1500–500	1155	1190–1130	Secondary amine, CN stretch
		1075 and 1014	1150–1000	Aliphatic fluoro compounds. C-F stretch
		868	800–860	Aromatic ring (para)
		770	770–735	Aromatic ring (ortho)

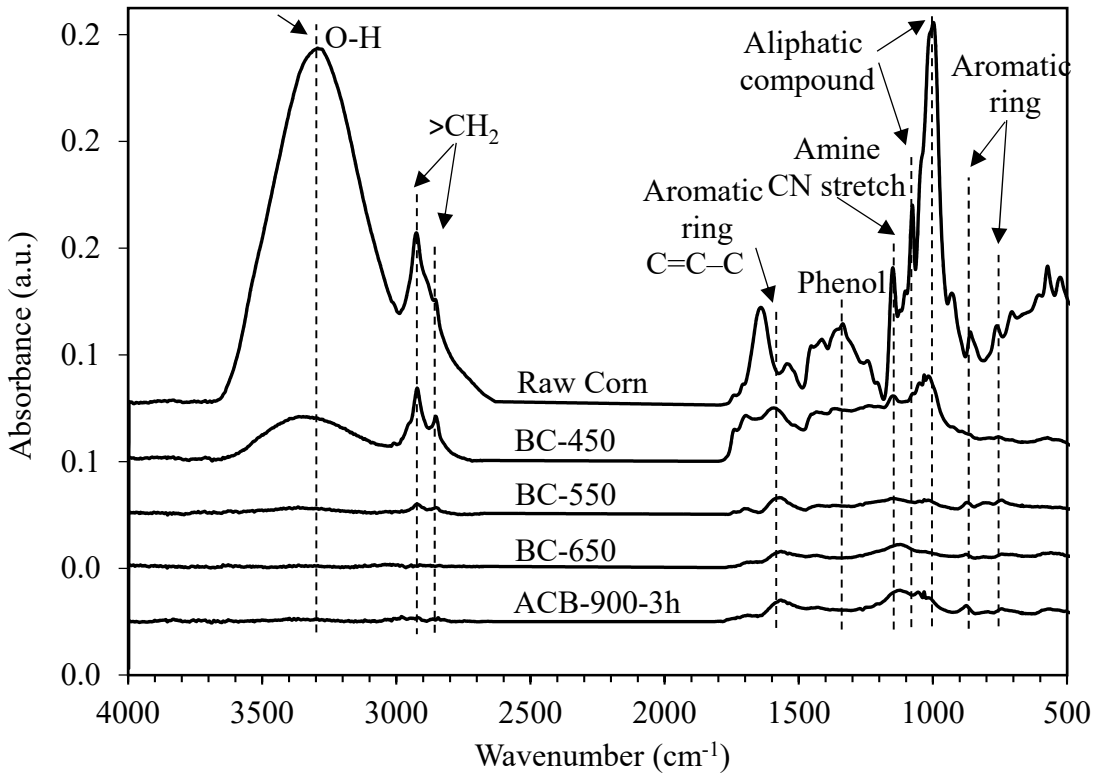

Figure 9. FTIR spectra of raw corn bio-char produced at 450, 550, and 650 °C (holding time: 30 min) and activated bio-char produced at 900 °C with activation holding time of 3 h.

3.4.3. BET Surface Area and Porosity Analysis

Table 9 indicates that the porosity and the BET surface area of the bio-char before activation is low. However, activating the bio-char (ACB) at 900 °C under CO_2 for 3 h significantly increases its specific surface area to 419 m^2g^{-1}. Furthermore, after activation, the pore volume of the biochar particles increased (from 0.003 to 0.23 cm^3g^{-1}) as shown in the SEM images (Figure 10). The activated bio-char's high surface area makes it a good candidate for the adsorption of contaminants from water, which will be investigated further in the next phase of this research.

Table 9. BET surface area and pore volume results for bio-char produced at 450, 550, and 650 °C and activated bio-char activated at 900 °C for 3 h.

Sample Name-Pyrolysis Temperature (°C)-Activation Time (Hour)	BET Surface Area (m^2g^{-1})	Pore Volume (cm^3g^{-1})
BC-450-0	0	0.003
BC-550-0	0.13	0.013
BC-650-0	2.84	0.01
ACB-500-3	419	0.23

3.4.4. SEM Images

The surface morphologies of raw corn, bio-chars, and activated bio-chars with magnitude ×500 are shown in the SEM images in Figure 10. Figure 10 illustrates that the raw corn surface is smooth and homogenous with no pores. SEM images show that the structure of corn changed from non-porous to a porous structure after pyrolysis. At 500 °C, some pores are detected; however, the presence of volatiles does not allow for the formation of more pores (Figure 10b). The results show that the size and quantity of pores developed by increasing the pyrolysis temperature (Figure 10c,d) can be attributed to further removing volatiles or organic matter from the char structure [25]. This finding is in agreement with the literature [31,32].

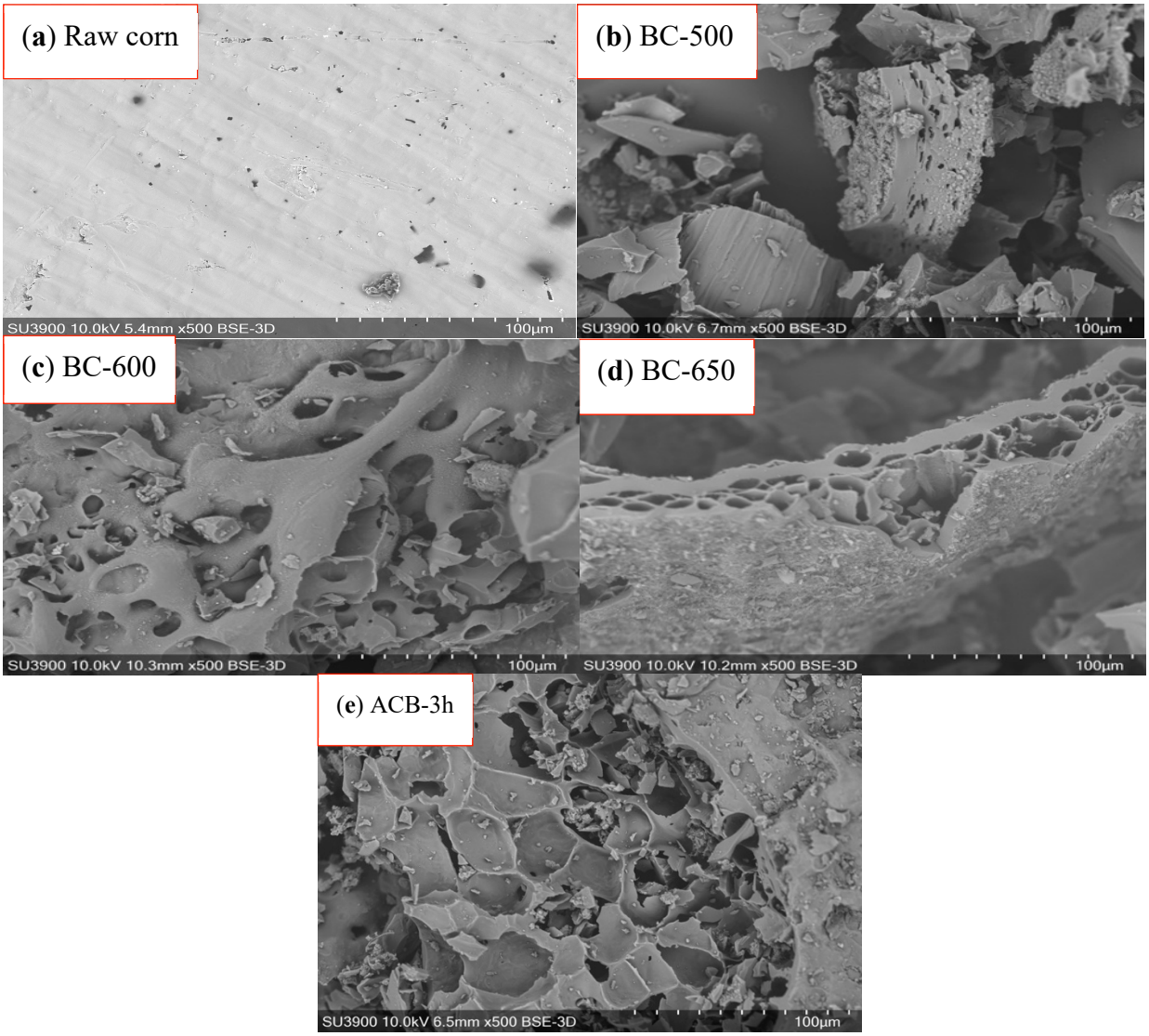

Figure 10. SEM images (500 magnitude) of (**a**) raw biomass, (**b**) bio-char at 500 °C, (**c**) bio-char at 600 °C, (**d**) bio-char at 650 °C, and (**e**) activated bio-chars produced at 900 °C with activation time of 3 h.

3.5. Non-Condensable Gases

The gas composition of four gas bag samples produced during the pyrolysis experiments was analyzed using a Micro-GC, and results are shown in Figure 11. Samples were collected at temperatures of 300, 400, 500, and 550 °C. Duplicate experiments confirmed the accuracy of the results. CO and CO_2 were present in the highest concentrations, followed by lower percentages of CH_4, H_2, and C_2H_4. The amount of H_2 increased with increasing temperatures, because more volatiles leave the structure of the biomass at higher temperatures. The gas-flow rates produced during pyrolysis were measured using a 100 mL bubble flow meter (purchased from Sigma-Aldrich, Oakville, ON, Canada) when the reactor had reached the pyrolysis temperatures of 300, 400, 500, and the final target temperature of 550 °C. The gas flow rates increased from 2 to 6 L min^{-1} between 300 and 500 °C and started decreasing after reaching 500 °C. No further gas was detected after 1 h (Figure 12). No significant gas production was noticeable before 300 °C. Moreover, the results show that most of the cracking products were generated between 300 and 500 °C, similarly to previously reported studies involving the cracking of starchy feedstocks [19,33].

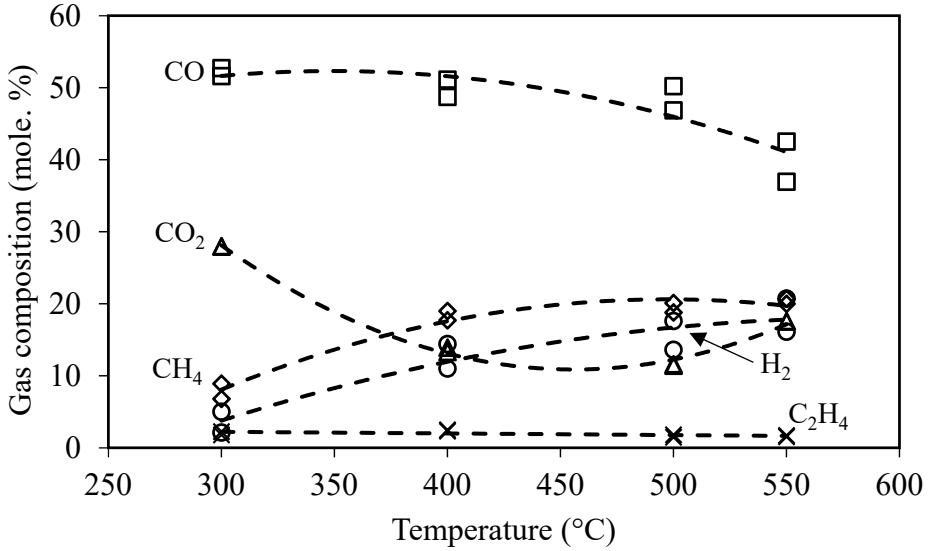

Figure 11. Gas composition of samples produced during pyrolysis collected at temperatures of 300, 400, 500, and the final temperature of 550 °C.

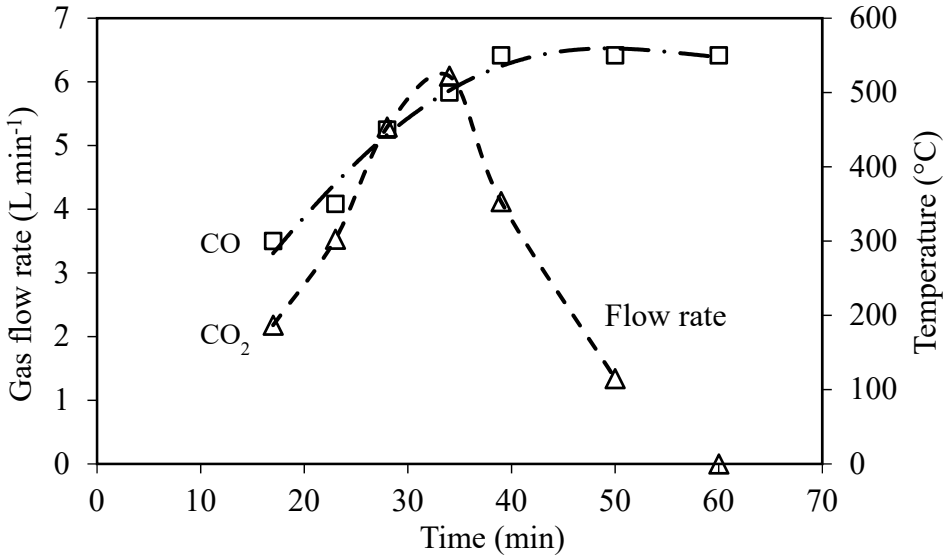

Figure 12. Gas-flow rate changes during the reaction time of 60 min at pyrolysis temperatures between 300 and 550 °C and heating rate of 20 °C min^{-1}.

The gas product is primarily used to provide heat to drive various processes, such as the pyrolysis process itself. The syngas could also be used to generate power, as other studies have shown [34]. Table 10 shows the calculated HHV. Comparing the HHV of the gas produced at the highest temperature (16.5 MJ/m^3) with that of town gas, which is 18 MJ/m^3, confirms the possible future applications of this product for energy production.

Table 10. HHV of gas stream at standard condition of T_r = 0 °C and P_r = 1 atm (NREL).

Temperature (°C)	HHV (MJ/Nm^3)
300	11.63
400	16.87
500	17.24
550	16.46

4. Conclusions

In this study, deoxynivalenol (DON) contaminated corn was converted into value-added products (e.g., bio-char, bio-oil, and gas) using slow pyrolysis in a batch reactor. The pyrolysis process reduced the DON concentration from 5–7 ppm in the raw corn grains to zero ppm, making thermochemical conversion a promising method for industrial applications. When the final reaction temperature increased from 450 °C to 650 °C, the bio-oil yield increased from 29 to 47 wt.%, while the bio-char yield decreased from 41 to 25 wt.%. The total gas yields were temperature independent and remained approximately constant (30%). The effect of the heating rate was investigated via testing between 5 and 35 °C min^{-1}. The result shows a maximum bio-oil yield of 46 wt.% which was achieved at the highest heating rates of 35 °C/min. Acetic acid and levoglucosan were the most significant components in the bio-oil, representing the highest GC-MS peaks, with yields of 26 and 13 g per kg of bio-oil. The pyrolysis operating temperature affected the pH of bio-char. For instance, the pH of the bio-char changed from 6.1 to 7.4 as the temperature increased from 450 to 650 °C. This is a promising result for soil amendment applications. The BET surface area of the bio-char significantly increased from 3 to 419 m^2 g^{-1} by activation at 900 °C in the presence of CO_2 for 3 h. The possible high adsorption capacity of activated bio-char could be due to the large number of pores developed during the activation process. This result was confirmed through SEM analysis. The presence of functional groups (e.g., –C=O, –C=N) on the biochar surface was confirmed with FTIR. The high pH (9) of the activated bio-char and the presence of functional groups make the activated corn bio-char a good candidate for adsorption applications. The gas product is comprised mainly of H_2, CO, CO_2, CH_4, and C_2H_4, and the HHV of this stream was calculated to be 16.46 MJ/Nm^3, showing its potential to be used as an energy source. The results show the potential industrial applications of bio-oil, activated bio-char, and non-condensable gases as chemicals, adsorbents, and energy resources, respectively.

Author Contributions: Conceptualization, F.B.; Data curation, S.K., S.P. and N.B.K.; Investigation, S.K., S.P., N.B.K. and F.B.; Methodology, S.K. and S.P.; Supervision, N.B.K. and F.B.; Writing—original draft, S.K.; Writing—review & editing, S.P., N.B.K. and F.B. All authors have read and agreed to the published version of the manuscript.

Funding: This research was funded by the Natural Sciences and Engineering Council of Canada (NSERC) and by the industry partners involved in the NSERC Industrial Research Chair program in "Thermochemical Conversion of Biomass and Waste to Bioindustrial Resources," grant number IRCPJ–537859.

Acknowledgments: This work has been generously supported by the Natural Sciences and Engineering Research Council of Canada (NSERC) and by the industry partners involved in the NSERC Industrial Research Chair program in "Thermochemical Conversion of Biomass and Waste to Bioindustrial Resources".

Conflicts of Interest: The authors declare no conflict of interest.

References

1. Khan, M.F.S.; Akbar, M.; Xu, Z.; Wang, H. A Review on the Role of Pretreatment Technologies in the Hydrolysis of Lignocellulosic Biomass of Corn Stover. *Biomass Bioenergy* **2021**, *155*, 106276. https://doi.org/10.1016/j.biombioe.2021.106276.
2. Serna-Saldivar, S.O. *Corn: Chemistry and Technology*; Elsevier: Amsterdam, The Netherlands, 2018; ISBN 978-0-12-811886-3.
3. Munkvold, G.P. Epidemiology of Fusarium Diseases and Their Mycotoxins in Maize Ears. In *Epidemiology of Mycotoxin Producing Fungi*; Xu, X., Bailey, J.A., Cooke, B.M., Eds.; Springer: Dordrecht, The Netherlands, 2003; pp. 705–713, ISBN 978-90-481-6387-8.
4. Wu, F.; Miller, J.D.; Casman, E.A. The Economic Impact of Bt Corn Resulting from Mycotoxin Reduction. *J. Toxicol. Toxin Rev.* **2004**, *23*, 397–424. https://doi.org/10.1081/TXR-200027872.
5. Sobrova, P.; Adam, V.; Vasatkova, A.; Beklova, M.; Zeman, L.; Kizek, R. Deoxynivalenol and Its Toxicity. *Interdiscip. Toxicol.* **2010**, *3*, 94–99. https://doi.org/10.2478/v10102-010-0019-x.
6. Mishra, S.; Srivastava, S.; Dewangan, J.; Divakar, A.; Kumar Rath, S. Global Occurrence of Deoxynivalenol in Food Commodities and Exposure Risk Assessment in Humans in the Last Decade: A Survey. *Crit. Rev. Food Sci. Nutr.* **2020**, *60*, 1346–1374. https://doi.org/10.1080/10408398.2019.1571479.

7. Center for Food Safety and Applied Nutrition; Center for Veterinary Medicine Guidance for Industry and FDA: Advisory Levels for Deoxynivalenol (DON) in Finished Wheat Products for Human Consumption and Grains and Grain By-Products Used for Animal Feed. Available online: https://www.fda.gov/regulatory-information/search-fda-guidance-documents/guidance-industry-and-fda-advisory-levels-deoxynivalenol-don-finished-wheat-products-human (accessed on 31 July 2010).
8. Rosser, B.; Tenuta, A. Ontario Grain Corn Ear Mould and Deoxynivalenol (DON) Mycotoxin Survey. 2020. Available online: https://fieldcropnews.com/2020/10/2020-ontario-grain-corn-ear-mould-and-deoxynivalenol-don-mycotoxin-survey/ (accessed on 13 October 2020).
9. Trenholm, H.L.; Charmley, L.L.; Prelusky, D.B.; Warner, R.M. Washing procedures using water or sodium carbonate solutions for the decontamination of three cereals contaminated with deoxynivalenol and zearalenone. *J. Agric. Food Chem.* **1992**, *40*, 2147–2151. https://doi.org/10.1021/jf00023a021.
10. Shinha, K.K.; Bhatnagar, D. *Mycotoxins in Agriculture and Food Safety*; CRC Press: Boca Raton, FL, USA, 1998; ISBN 978-0-8247-0192-5.
11. Bullerman, L.B.; Bianchini, A. Stability of Mycotoxins during Food Processing. *Int. J. Food Microbiol.* **2007**, *119*, 140–146. https://doi.org/10.1016/j.ijfoodmicro.2007.07.035.
12. Cazzaniga, D.; Basilico, J.C.; Gonzalez, R.J.; Torres, R.L.; de Greef, D.M. Mycotoxins Inactivation by Extrusion Cooking of Corn Flour. *Lett. Appl. Microbiol.* **2001**, *33*, 144–147. https://doi.org/10.1046/j.1472-765x.2001.00968.x.
13. Krstović, S.; Krulj, J.; Jakšić, S.; Bočarov-Stančić, A.; Jajić, I. Ozone as Decontaminating Agent for Ground Corn Containing Deoxynivalenol, Zearalenone, and Ochratoxin A. *Cereal Chem.* **2021**, *98*, 135–143. https://doi.org/10.1002/cche.10289.
14. Young, J.C. Reduction in Levels of Deoxynivalenol in Contaminated Corn by Chemical and Physical Treatment. *J. Agric. Food Chem.* **1986**, *34*, 465–467. https://doi.org/10.1021/jf00069a022.
15. El-Sayed, S.A.; Mostafa, M.E. Pyrolysis Characteristics and Kinetic Parameters Determination of Biomass Fuel Powders by Differential Thermal Gravimetric Analysis (TGA/DTG). *Energy Convers. Manag.* **2014**, *85*, 165–172. https://doi.org/10.1016/j.enconman.2014.05.068.
16. Chen, T.; Liu, R.; Scott, N.R. Characterization of Energy Carriers Obtained from the Pyrolysis of White Ash, Switchgrass and Corn Stover—Biochar, Syngas and Bio-Oil. *Fuel Process. Technol.* **2016**, *142*, 124–134. https://doi.org/10.1016/j.fuproc.2015.09.034.
17. Papari, S.; Hawboldt, K. A Review on the Pyrolysis of Woody Biomass to Bio-Oil: Focus on Kinetic Models. *Renew. Sustain. Energy Rev.* **2015**, *52*, 1580–1595. https://doi.org/10.1016/j.rser.2015.07.191.
18. Bridgwater, A.V. Review of Fast Pyrolysis of Biomass and Product Upgrading. *Biomass Bioenergy* **2012**, *38*, 68–94. https://doi.org/10.1016/j.biombioe.2011.01.048.
19. Qiao, Y.; Wang, B.; Ji, Y.; Xu, F.; Zong, P.; Zhang, J.; Tian, Y. Thermal Decomposition of Castor Oil, Corn Starch, Soy Protein, Lignin, Xylan, and Cellulose during Fast Pyrolysis. *Bioresour. Technol.* **2019**, *278*, 287–295. https://doi.org/10.1016/j.biortech.2019.01.102.
20. Wang, Y.; Akbarzadeh, A.; Chong, L.; Du, J.; Tahir, N.; Awasthi, M.K. Catalytic Pyrolysis of Lignocellulosic Biomass for Bio-Oil Production: A Review. *Chemosphere* **2022**, *297*, 134181. https://doi.org/10.1016/j.chemosphere.2022.134181.
21. Cheng, F.; Bayat, H.; Jena, U.; Brewer, C.E. Impact of Feedstock Composition on Pyrolysis of Low-Cost, Protein- and Lignin-Rich Biomass: A Review. *J. Anal. Appl. Pyrolysis* **2020**, *147*, 104780. https://doi.org/10.1016/j.jaap.2020.104780.
22. Barry, D.J. Pyrolysis as an Economical and Ecological Treatment Option for Solid Anaerobic Digestate and Municipal Sewage Sludge. Master's Thesis, The University of Western Ontario, London, ON, Canada, 2018; p. 94.
23. Parvulescu, O.C.; Dobre, T.; Ceatra, L.; Iavorshi, G.; Mirea, R. Characteristics of Corn Grains Pyrolysis in a Fixed Bed Reactor. *Rev. Chim.* **2011**, *6*, 89–94.
24. Yang, Z.; Liu, X.; Yang, Z.; Zhuang, G.; Bai, Z.; Zhang, H.; Guo, Y. Preparation and Formation Mechanism of Levoglucosan from Starch Using a Tubular Furnace Pyrolysis Reactor. *J. Anal. Appl. Pyrolysis* **2013**, *102*, 83–88. https://doi.org/10.1016/j.jaap.2013.03.012.
25. Naik, D.K.; Monika, K.; Prabhakar, S.; Parthasarathy, R.; Satyavathi, B. Pyrolysis of sorghum bagasse biomass into bio-char and bio-oil products: A Thorough Physicochemical Characterization. *J. Therm. Anal.* **2017**, *127*, 1277–1289. https://doi.org/10.1007/s10973-016-6061-y.
26. Schwietzke, S.; Kim, Y.; Ximenes, E.; Mosier, N.; Ladisch, M. Ethanol Production from Maize. In *Molecular Genetic Approaches to Maize Improvement*; Kriz, A.L., Larkins, B.A., Eds.; Springer: Berlin/Heidelberg, Germany, 2009; Volume 63, pp. 347–364 ISBN 978-3-540-68919-5.
27. Oromiehie, A.R.; lari, T.T.; Rabiee, A. Physical and Thermal Mechanical Properties of Corn Starch/LDPE Composites. *J. Appl. Polym. Sci.* **2013**, *127*, 1128–1134. https://doi.org/10.1002/app.37877.
28. Zhao, J.; Shen, X.-J.; Domene, X.; Alcañiz, J.-M.; Liao, X.; Palet, C. Comparison of Biochars Derived from Different Types of Feedstock and Their Potential for Heavy Metal Removal in Multiple-Metal Solutions. *Sci. Rep.* **2019**, *9*, 9869. https://doi.org/10.1038/s41598-019-46234-4.
29. Kizil, R.; Irudayaraj, J.; Seetharaman, K. Characterization of Irradiated Starches by Using FT-Raman and FTIR Spectroscopy. *J. Agric. Food Chem.* **2002**, *50*, 3912–3918. https://doi.org/10.1021/jf011652p.
30. Nandiyanto, A.B.D.; Oktiani, R.; Ragadhita, R. How to Read and Interpret FTIR Spectroscope of Organic Material. *Indones. J. Sci. Technol.* **2019**, *4*, 97. https://doi.org/10.17509/ijost.v4i1.15806.

31. Neder-Suárez, D.; Amaya-Guerra, C.A.; Pérez-Carrillo, E.; Quintero-Ramos, A.; Mendez-Zamora, G.; Sánchez-Madrigal, M.Á.; Barba-Dávila, B.A.; Lardizábal-Gutiérrez, D. Optimization of an Extrusion Cooking Process to Increase Formation of Resistant Starch from Corn Starch with Addition of Citric Acid. *Starch* **2020**, *72*, 1900150. https://doi.org/10.1002/star.201900150.
32. Hernández-Becerra, E.; Jimenez, B.L.C.; Vuelvas-Solorzano, A.; Millan-Malo, B.; Muñoz-Torres, C.; Toledo, M.O.; Rodriguez-Garcia, M.E. Physicochemical and morphological changes in corn grains and starch during the malting for Palomero and Puma varieties. *Cereal Chem.* **2020**, *97*, 404–415. https://doi.org/10.1002/cche.10256.
33. Abdullah, A.H.D.; Chalimah, S.; Primadona, I.; Hanantyo, M.H.G. Physical and chemical properties of corn, cassava, and potato starchs. *IOP Conf. Series Earth Environ. Sci.* **2018**, *160*, 012003. https://doi.org/10.1088/1755-1315/160/1/012003.
34. Sharma, P.; Sahoo, B.B. An ANFIS-RSM based modeling and multi-objective optimization of syngas powered dual-fuel engine. *Int. J. Hydrogen Energy* **2022**, *47*, 19298–19318. https://doi.org/10.1016/j.ijhydene.2022.04.093.